JATIS Journal of Astronomical Telescopes, Instruments, and Systems

RESEARCH PAPER

Focal plane of the Arcus Probe X-ray spectrograph

Catherine E. Grant,[a,*] **Marshall W. Bautz**,[a] **Eric D. Miller**,[a] **Richard F. Foster**,[a] **Beverly LaMarr**,[a] **Andrew Malonis**,[a] **Gregory Prigozhin**,[a] **Benjamin Schneider**,[a] **Christopher Leitz**,[b] **and Abraham D. Falcone**[c]

[a]Massachusetts Institute of Technology, Kavli Institute for Astrophysics and Space Research, Cambridge, Massachusetts, United States

[b]Massachusetts Institute of Technology, Lincoln Laboratory, Lexington, Massachusetts, United States

[c]Pennsylvania State University, Department of Astronomy and Astrophysics, University Park, Pennsylvania, United States

ABSTRACT. The Arcus Probe mission concept provides high-resolution soft X-ray and ultraviolet spectroscopy to reveal feedback-driven structure and evolution throughout the universe with an agile response capability ideal for probing the physics of time-dependent phenomena. The X-ray spectrograph utilizes two nearly identical charge-coupled device (CCD) focal planes to detect and record X-ray photons from the dispersed spectra and zero-order of the critical angle transmission gratings. We describe the Arcus focal plane instrument and the CCDs, including laboratory performance results, which meet the observatory requirements.

Keywords: Arcus; X-ray detectors; X-ray spectroscopy; charge-coupled devices

Paper 24079SS received Jun. 3, 2024; revised Sep. 30, 2024; accepted Oct. 11, 2024; published Nov. 8, 2024.

1 Introduction

The Arcus Probe mission concept, submitted to the National Aeronautics and Space Administration (NASA) Astrophysics Probe Explorer proposal call with an expected launch in the early 2030s, will explore the formation and evolution of clusters, galaxies, and stars through high-resolution X-ray and ultraviolet (UV) spectroscopy. Arcus can reveal feedback-driven structure and evolution throughout the universe due to advances in optics and high-resolution gratings which enable breakthrough science.[1] The Arcus mission includes two co-aligned instruments working simultaneously to provide high-resolution spectra in both the soft X-ray (12 to 50 Å; 0.25 to 1 keV; $R > 2500$) and far UV (1020 to 1540 Å; $R > 17{,}000$), with an agile response capability to address time-domain science (response to target of opportunity triggers in as little as 4 h).

The Arcus X-ray spectrograph (XRS) consists of four parallel, almost identical optical channels that feed two detector focal plane arrays, which record both the dispersed spectra and the zero-order of the gratings. Each optical channel consists of silicon pore optics,[2] identical to the design of the NewAthena optics, and critical-angle transmission gratings.[3] The optics plus gratings are separated from the detectors by a 10-m-long coilable boom, enclosed within a sock to suppress stray light. The rear of the spacecraft holds two charge-coupled device (CCD) detector assemblies which detect and record the diffracted X-ray photons. For a given optical channel, the zero-order image and low diffraction orders fall on one detector array, whereas the high orders fall on the other—two channels on one side and two channels in the reverse direction. The optical

*Address all correspondence to Catherine Grant, cgrant@mit.edu

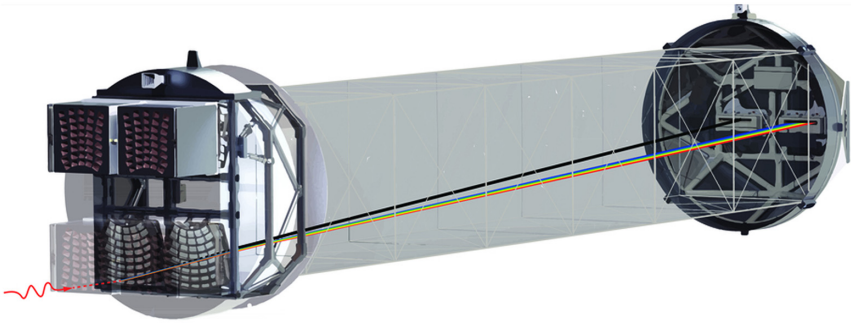

Fig. 1 Rendering of the Arcus XRS after deployment. At the left, the front assembly holds the four optical channels, two of which are shown with their thermal pre-colimators (left, top) and open doors, whereas the other two (left, bottom) have these removed to show the silicon pore optics mounted in their petal structure. Each petal holds 40 mirror modules in eight rows, with an (unseen) grating petal mounted behind it. The extendable boom connects the front assembly to the rear assembly that holds two CCD focal planes and their associated electronics. The boom is wrapped with a light-tight sock to suppress stray light (from Ref. 1).

channels are offset from each other in the cross-dispersion direction, so as not to overlap on the detector. The CCD energy resolution is used to differentiate the co-spatial diffraction orders. A rendering of the XRS after deployment is shown in Fig. 1.

Section 2 introduces the XRS focal plane instrument, whereas Sec. 3 further details the CCDs. Ground testing of the CCDs designed for Arcus XRS is presented in Sec. 4. The Arcus mission[1] and the UV spectrograph[4,5] are further described elsewhere and in this special section of *JATIS*.

2 XRS Instrument Detector Subsystem

The XRS Instrument Detector Subsystem (IDS) contains the detector array CCDs and their associated electronics and structures which detect the X-ray photons focused and dispersed by the optics and gratings. The IDS consists of two detector assemblies (DA), each with eight CCDs, and two associated detector electronics (DE) boxes. Each DA+DE pair operates independently and in parallel. The IDS records diffracted and zero-order photons and sends the digitized pixel pulse height data to the event recognition processor (ERP) in the XRS instrument control unit (XICU) where the raw data are processed and sent to the spacecraft for downlink to the ground. Some basic characteristics of the XRS focal plane are shown in Table 1.

2.1 Detector Assembly

Renderings of an individual Arcus CCD in the flight package and an XRS detector assembly focal plane are shown in Figs. 2 and 3. Eight CCDs are arranged in a linear array along the dispersion direction of the gratings. The CCDs are tilted to best match the curved focal surface.

Table 1 XRS focal plane characteristics.

Detectors	Frame transfer X-ray CCDs
Focal plane array	8-CCD array per detector assembly
CCD spectral resolution requirement	FWHM < 70 eV at 0.5 keV
System read noise requirement	$\leq 4e^-$ RMS at 625 kpixels/s
CCD frame rate	1 Hz
Focal plane temperature	-90 ± 0.5°C
Optical blocking filter	40 nm Al on-chip
Contamination blocking filter	45 nm polyimide + 30 nm Al

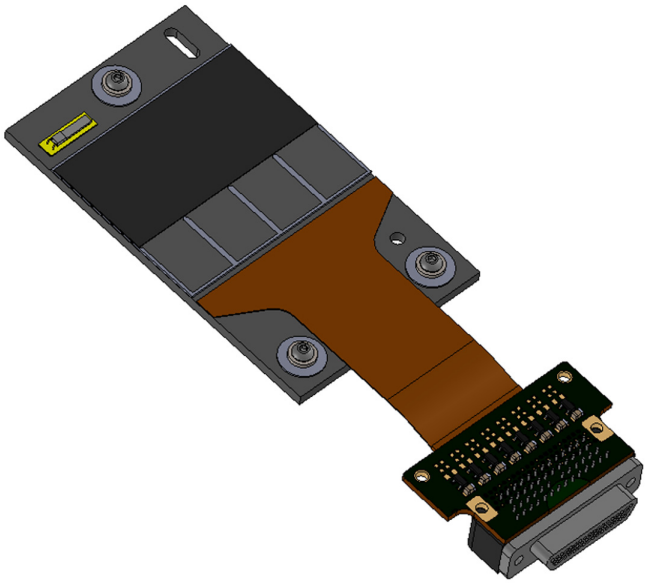

Fig. 2 Arcus MIT Lincoln Laboratory CCID-94 back-illuminated CCD in a flight package. The dark rectangle is the imaging area of the CCD; the grey smaller rectangles are the frame store areas. Each detector assembly has eight such CCDs.

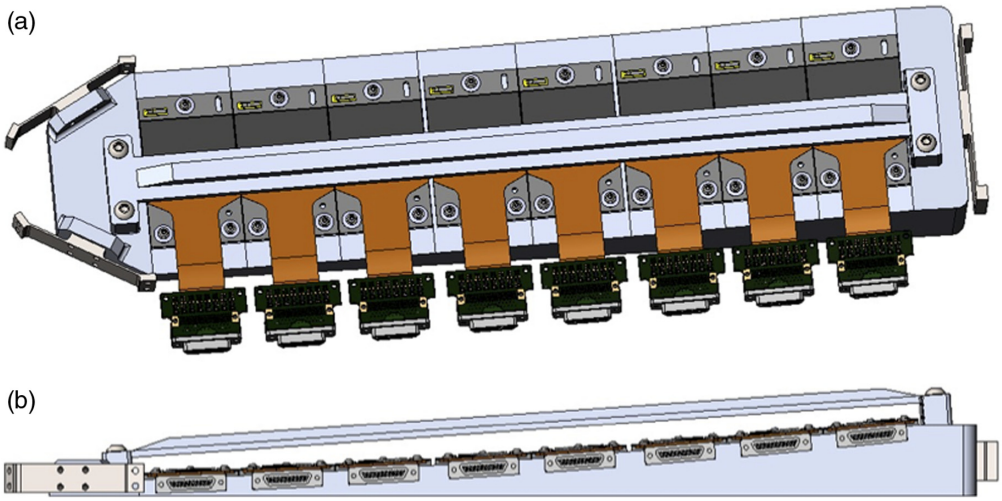

Fig. 3 Eight Arcus CCDs in a detector assembly focal plane arranged linearly along the dispersion direction of the gratings. (a) Viewed from above, as seen by the optics. (b) Viewed from the side. The frame store region is shielded by an aluminum cover. Each CCD is tilted to best match the curved focal surface. Arcus contains two detector assemblies to read out the four optical channels.

Gaps between the CCDs are minimized (∼2 mm between active areas). The alignment with the XRS optics has been optimized to ensure that of the four optical channels, no two spectra have chip gaps at the same wavelength. An aluminum cover shields the frame store region from X-ray interactions during readout.

The detector assembly focal planes are each enclosed in a housing that provides structural support for the CCDs, thermal and electrical connections, and a controlled environment. The detector housing is shown in Fig. 4. The aluminum housing provides 5 $\mathrm{gm\,cm^{-2}}$ of (spherically averaged) radiation shielding, which meets the Arcus lifetime requirement for the mitigation of radiation damage and minimization of charge transfer inefficiency (CTI) increase. An analysis of the effect of shielding on the in-band particle background will be done as part of a future study. The CCDs are passively cooled via a radiator with active heater control to maintain -90 ± 0.5°C.

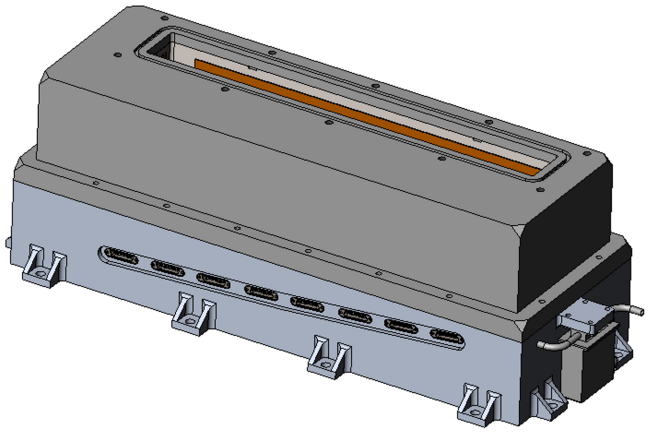

Fig. 4 One of two Arcus detector assemblies with the focal plane CCDs enclosed by the housing. X-rays enter through the long slot at the top of the housing and pass through the contamination blocking filter, just inside. The door, which maintains a vacuum within the housing and is opened once after launch, is not shown.

A door preserves the vacuum within the housing to protect the focal plane from molecular contamination and is opened once post-launch after sufficient time for the rest of the spacecraft to outgas.

Contamination blocking filters (CBFs) are mounted inside the housing to protect the cold detectors from accumulating molecular contamination which would reduce the XRS effective area by absorbing low-energy X-rays. The CBF also provides optical light blocking. The temperature of the CBF is maintained above $+20$°C by heater control to prevent contamination of the filters. The CBF consists of a metal mesh supporting 45-nm polyimide and 30-nm aluminum and is in vacuum at launch to prevent any damage due to acoustic loading.

Optical stray light on the CCD focal plane would degrade the X-ray photon energy measurement required for order sorting by producing additional time- and position-varying background noise. A series of design elements mitigates stray light. The XRS boom is surrounded by a 25-μm-thick sock which limits stray light into the optical bench. A baffle limits the view of each DA to the optics. Finally, the CBF and on-chip optical blocking filter (OBF) attenuate any remaining visible/infrared stray light to 10 ppm of the incoming flux.

The CCD response (gain, line width, and quantum efficiency) will be calibrated at the Massachusetts Institute of Technology before integration into the full XRS using protocols developed for Chandra ACIS and Suzaku XIS, with X-ray line sources from 0.5 to 6 keV.[6–8] Prelaunch end-to-end X-ray testing of the XRS will verify system performance. Changes in the CCD gain after launch will be tracked by collimated ^{55}Fe sources in each DA housing which produce X-rays at 5.9 and 6.4 keV from Mn-Kα and Kβ. These are mounted to continuously illuminate the top portion of all CCDs outside of the region where the dispersed spectra are detected. This scheme was successfully used on Suzaku to monitor the changes in the CCD performance, measure CTI, and calibrate gain.

2.2 Detector Electronics

Each detector assembly has a corresponding DE box that drives and reads out the CCDs, transmitting the digitized pixel data onto the XICU. Each DE contains eight identical focal plane electronics boards (FPEBs), one per CCD, along with an interface board, thermal control board, and power distribution board.

The FPEBs provide programmable analog clock waveforms and biases to operate the CCDs, as well as low-noise analog signal processing and digitization of the output signal. The FPEB clock drivers consist of complementary metal-oxide-semiconductor (CMOS)-level translators followed by discrete current amplifiers. A programmable sequencer provides CCD clock and analog processor timing. The low-voltage analog design reduces power and distortion and allows lower impedances for low thermal Johnson noise and cross-talk. The CCD readout sequence and clock levels are configurable on orbit. The circuitry has heritage from Chandra ACIS and Suzaku

XIS, with a low total readout noise of $<4\ e^-$ which minimizes the noise contribution to the CCD energy resolution, required to separate the spatially coincident diffraction orders. Low noise also ensures the detection of X-ray events at the low-energy end of the Arcus passband (0.25 keV). Each board has a dedicated analog processing chain serving the eight independent CCD outputs per chip. The 1-s frame time ensures negligible pile-up in the dispersed spectra.

The DE interface board provides a command and telemetry interface between the XICU and the FPEBs. The interface board produces a stream of digitized pixel data from the CCDs and FPEBs, which is sent on to the XICU for event finding and filtering, as well as sending science and engineering housekeeping information. Regulated power is provided to the FPEBs by the power distribution board, whereas the thermal control board regulates the temperature of the focal plane and the CBF to -90°C and $+20$°C, respectively.

2.3 XRS Instrument Control Unit

The activities of the XRS are controlled by the XICU, which is responsible for gathering and storing all XRS data for transfer to the spacecraft. A key component of the XICU is the ERP, which reads in the digitized pixel pulse heights from the CCDs and extracts candidate X-ray events, reducing the data rate by many orders of magnitude.[9] The ERP uses the same event recognition algorithms employed on Chandra, Swift, and Suzaku, bias-correcting the pixel stream passed from the DE, then identifying local maxima as candidate events and storing the position, time, and pulse height values for a 3×3 pixel event island, for packaging into telemetry. The ERP implements event processing in firmware rather than software, achieving much higher data processing speeds than legacy missions, required for the large 32-megapixel Arcus focal plane. The design and implementation of a prototype field programmable gate array (FPGA)-based ERP are described in Ref. 9 and the measured performance of the prototype is sufficient to meet the needs of the Arcus XRS focal plane.

3 XRS CCDs

The Arcus CCDs are CCID-94 backside-illuminated (BI) frame transfer devices designed and manufactured specifically for Arcus by MIT Lincoln Laboratory (MIT/LL). Some of their characteristics are listed in Table 2. They derive directly from the CCID-41 devices, which performed as designed throughout the 10-year Suzaku mission, and the CCID-17 devices, which are still operating on Chandra more than 24 years after launch. X-ray photons interact in the depleted silicon, producing photoelectrons that drift into the buried channel under the influence of an applied electric field. After the 1-s integration time, the charge packets are quickly transferred

Table 2 XRS CCD characteristics.

Detectors	Back-illuminated frame transfer CCDs
Format	2048×1024 pixel imaging array
Image area pixel size	$24 \times 24\ \mu$m
Die size	5×4 cm
Output ports	8 two-stage pJFETs
Transfer gate design	Triple-layer polysilicon
Radiation tolerance features	Trough, charge injection
Detector thickness	50 μm (fully depleted)
Back surface passivation	Molecular beam epitaxy 10 nm
Typical serial rate	0.5 MHz
Typical parallel rate	0.1 MHz
Full frame rate	1 Hz

into the frame store region and then more slowly transferred through the serial register to one of eight output ports to be amplified and read out.

The CCID-94 shares many design features of its predecessor BI detectors: 24 μm pixel size, 50 μm thickness (fully depleted), three-phase charge transfer through triple-layer polysilicon transfer gates, three-side abuttability, and frame store design. The CCID-94 is capable of charge injection, which has been very effective at mitigating charge transfer inefficiency due to radiation damage on Suzaku XIS.[10,11] The Arcus devices are twice as wide as the Chandra and Suzaku devices, 2048 pixels compared with 1024, to better cover the grating dispersion pattern and have twice as many parallel output amplifiers to maintain sufficiently fast readout speed for preventing photon pile-up while ensuring low readout noise.

The single-stage on-chip metal-oxide-semiconductor field-effect transistor (MOSFET) used in Chandra and Suzaku has been replaced by a high-bandwidth, high-responsivity two-stage p-channel junction field effect transistor (pJFET) amplifier. This allows up to 10 times faster readout speeds while maintaining low readout noise. Arcus requires a 1-s CCD frame time to minimize pile-up, which is easily met by the baseline 625-kHz serial readout rate. The CCD backside

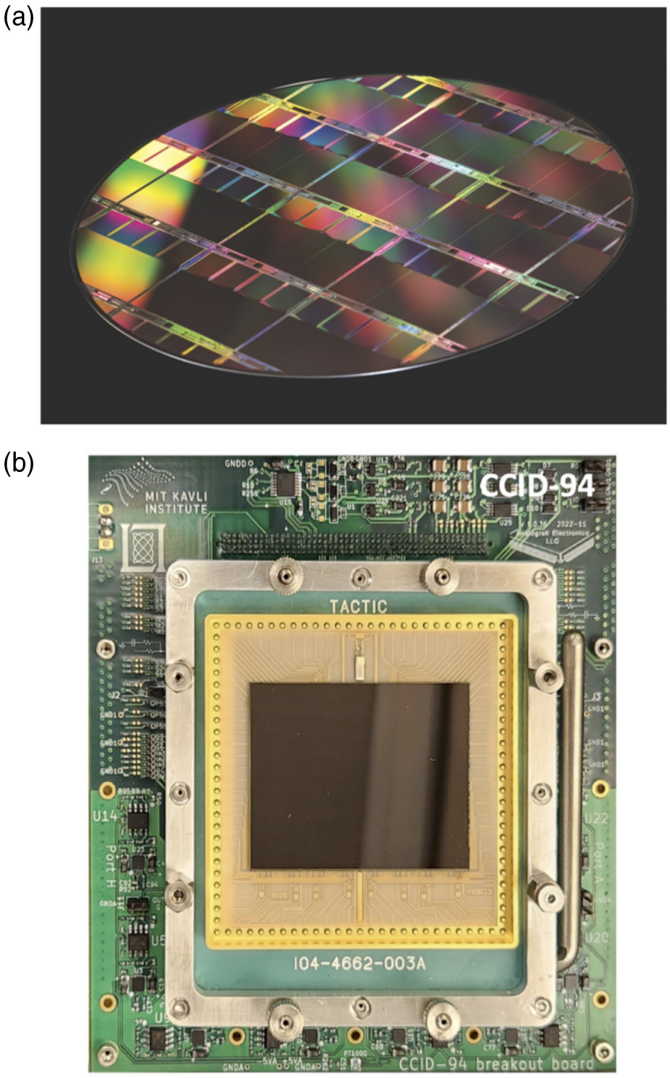

Fig. 5 (a) Photograph of MIT/LL CCID-94 wafer before packaging. The large rectangular imaging area and smaller rectangular frame store arrays of each CCD are visible as the wafer is viewed from the front illuminated side. (b) Photograph of a packaged MIT/LL CCID-94 undergoing testing for Arcus development and performance demonstration at MKI. The frame store cover is not installed. As the device is back-illuminated, the structures defining the imaging and frame store arrays cannot be seen. The eight readout chains are visible at the bottom of the device.

is passivated with a molecular beam epitaxy process that deposits a 10-nm layer of heavily doped silicon. The CCDs also feature a 40-nm directly deposited aluminum blocking filter, which works in conjunction with the CBF to prevent stray optical light from producing additional noise in the detectors.[12]

4 CCD X-Ray Performance

The development of advanced, fast-readout CCD detectors for future missions has been undertaken by our groups at MIT/LL and the MIT Kavli Institute (MKI) for the past several years, most recently reported in Refs. 13 and 14. Photographs of the CCID-94 device, designed specifically for the Arcus XRS, are shown at the wafer level (front-illuminated) and after packaging for lab testing (back-illuminated) in Fig. 5. The CCDs tested in the lab do not have the on-chip optical blocking layer that is planned for the flight devices.

The MKI facility used for X-ray performance testing of the CCID-94 is described more fully in Ref. 14. Test CCDs in a vacuum chamber with a liquid nitrogen cryostat can be illuminated by a variety of X-ray line sources, including radioactive ^{55}Fe producing Mn-Kα and Kβ fluorescence lines at 5.9 and 6.4 keV, respectively, and a radioactive ^{210}Po source fluorescing a Teflon target producing lines of C-K (0.25 keV) and F-K (0.7 keV). In addition, there is an in-focus monochromator (IFM) which produces clean monochromatic lines at energies below 2 keV.[15]

The measured readout noise is low and uniform across the device, ranging from 2 to 3e^- root mean square (RMS), well below the 4e^- readout noise requirement. The spectral resolution is also excellent across the Arcus energy bandwidth. Figure 6 demonstrates CCID-94 full width at half maximum (FWHM) performance using a combination of the two radioactive sources. The serial and parallel clocking rates and the CCD temperature were all consistent with those planned for Arcus. The data have been processed in a similar fashion as would be done on-board: finding candidate X-ray events, recording a 3×3 pixel event island, and calculating the event energies. Each event is assigned a pixel "multiplicity," akin to the "grade" on Chandra and Suzaku, to indicate the number of pixels in an event island that is above the threshold. We include multiplicities up to four in our results. The measured FWHM at 0.7 keV is 66 eV, which meets the Arcus low energy spectral resolution requirement of 70 eV with similar performance on all eight nodes of the device. A small non-Gaussian tail develops at energies below 1 keV, which may be due to incomplete charge collection due to losses at the surface of the CCD but represents <10% of the photon counts in the line at 0.7 keV. This feature is currently under further investigation which will be reported in a future paper.

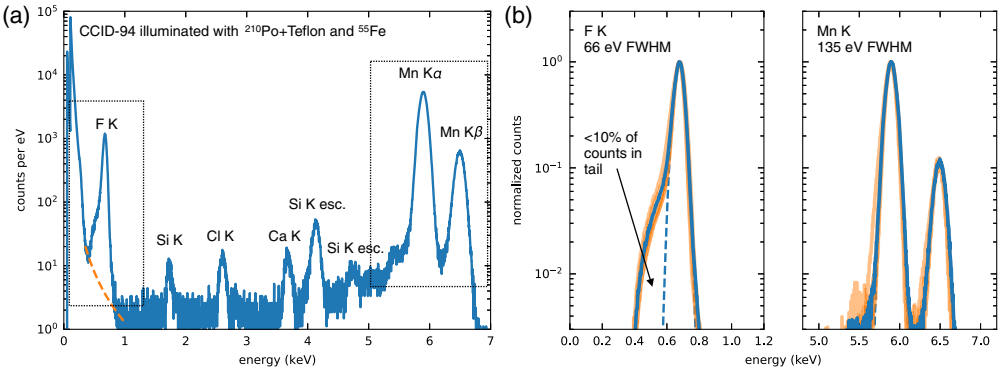

Fig. 6 (a) Spectrum of a single CCID-94 segment (node "C") simultaneously illuminated by ^{210}Po with a Teflon target and ^{55}Fe. The primary fluorescence lines of F-K, Mn-Kα, and Mn-Kβ can be seen along with several other fluorescence and escape features. (b) Zoom-in of the F-K and Mn-K peaks from panel (a), now also showing spectra from the other seven nodes of this device in orange. The F-K line has been corrected for the noise continuum by subtracting a best-fit power law, shown in dashed orange in panel (a). Gaussian fits (dashed blue lines) indicate that the FWHM meets the Arcus spectral resolution requirement. Although the F-K peak shows a non-Gaussian tail, it contains fewer than 10% of the line counts. These results include events with pixel multiplicities up to four.

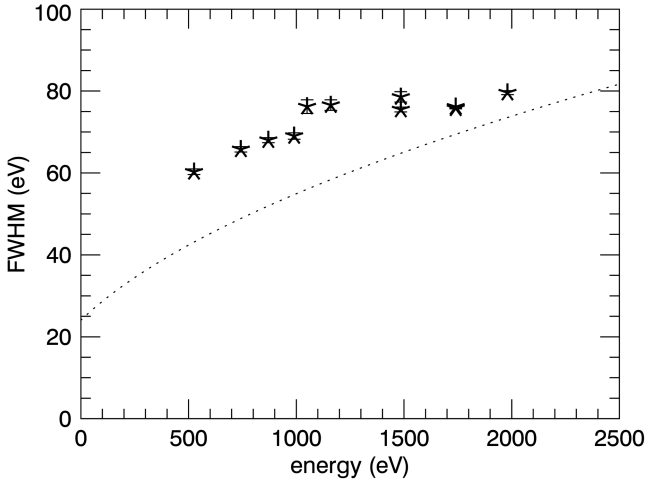

Fig. 7 Spectral FWHM for the CCID-94 as a function of X-ray line energy as measured by the IFM. The dotted line is the theoretical best possible FWHM assuming the measured noise for this output node ($2e^-$) and a simplified model of event splitting. The Arcus requirement of FWHM < 70 eV at 0.5 keV is clearly met by this device. These results include events with pixel multiplicities up to four as is typical for Chandra and Suzaku.

A second demonstration of the CCID-94 performance was done with the IFM, measuring the FWHM at several X-ray energies from 0.5 to 2 keV. This is shown in Fig. 7, where the spectral FWHM remains below the Arcus requirement up to ∼1 keV.

5 Summary

The Arcus Probe mission concept will provide high-resolution X-ray and UV spectroscopy to explore a wide range of science topics. The X-ray spectrograph provides substantial improvement in sensitivity and resolution over anything flown previously. The XRS focal plane utilizes high-heritage MIT/LL CCDs with proven technologies to read out the diffracted photons. Lab testing confirms CCID-94 performance more than meets the required CCD spectral resolution and read out noise for low-energy sensitivity and order sorting of the grating photons.

Disclosures

The authors of this paper are members of the Arcus collaboration. Should NASA select Arcus for implementation, their institutions will receive funding which may be used to fund the author's salaries in full or in part in the future.

Code and Data Availability

The data that support the findings of this article are not publicly available. They can be requested from the author at cgrant@mit.edu.

Acknowledgments

We gratefully acknowledge support from NASA through the Strategic Astrophysics Technology (SAT) Program (Grant Nos. 80NSSC19K0401 and 80NSSC22K0788) and from the Kavli Research Infrastructure Fund of the MIT Kavli Institute for Astrophysics and Space Research. We thank the reviewers for their helpful comments.

References

1. R. Smith, "The Arcus Probe mission," *Proc. SPIE* **12678**, 126780E (2023).
2. D. Girou et al., "Silicon pore optics: a mature and adaptable X-ray mirror technology," *Proc. SPIE* **12679**, 1267905 (2023).
3. R. K. Heilmann et al., "Soft X-ray performance and fabrication of flight-like blazed transmission gratings for the X-ray spectrometer on Arcus Probe," *Proc. SPIE* **12679**, 126790L (2023).

4. K. France et al., "Far-ultraviolet spectroscopy on the Arcus X-ray probe," *Proc. SPIE* **12678**, 126780F (2023).
5. B. T. Fleming et al., "The Arcus ultraviolet spectrograph (UVS): technical design of the far-ultraviolet spectrograph on the Arcus Probe," *Proc. SPIE* **12678**, 126780G (2023).
6. M. W. Bautz et al., "X-ray CCD calibration for the AXAF CCD imaging spectrometer," *Proc. SPIE* **2808**, 170–181 (1996).
7. M. W. Bautz et al., "Absolute calibration of ACIS X-ray CCDs using calculable undispersed synchrotron radiation," *Proc. SPIE* **4012**, 53–67 (2000).
8. B. LaMarr et al., "Ground calibration of X-ray CCD detectors with charge injection for the X-ray imaging spectrometer on Astro-E2," *Proc. SPIE* **5501**, 385–391 (2004).
9. D. N. Burrows et al., "Fast event recognition for X-ray silicon imagers," *Proc. SPIE* **9905**, 99050L (2016).
10. M. W. Bautz et al., "Mitigating CCD radiation damage with charge injection: first flight results from Suzaku," *Proc. SPIE* **6686**, 66860Q (2007).
11. H. Nakajima et al., "Performance of the charge-injection capability of Suzaku XIS," *PASJ* **60**, S1–S9 (2008).
12. M. Bautz et al., "Directly-deposited blocking filters for high-performance silicon X-ray detectors," *Proc. SPIE* **9905**, 99054C (2016).
13. M. Bautz et al., "Performance of high frame-rate X-ray CCDs for future strategic missions," *Proc. SPIE* **12181**, 121812A (2022).
14. E. D. Miller et al., "The high-speed X-ray camera on AXIS," *Proc. SPIE* **12678**, 1267816 (2023).
15. M. C. Hettrick, "In-focus monochromator: theory and experiment of a new grazing incidence mounting," *Appl. Opt.* **29**, 4531–4535 (1990).

Catherine E. Grant received her bachelor's degree in astronomy and astrophysics from Harvard University in 1993 and her PhD in astronomy and astrophysics from Penn State University in 1999. She is currently a research scientist at the MIT Kavli Institute for Astrophysics and Space Research. Her role includes characterizing radiation damage in the Chandra ACIS CCDs, developing software techniques for mitigating charge transfer inefficiency and flight software algorithms to allow ACIS to act as its own radiation monitor, and efforts to reduce and understand the particle background in future X-ray missions using *in situ* particle data and Geant4 simulations.

Biographies of the other authors are not available.